

The Molecular Structure of Trimethylphosphine-Boron Triiodide as Studied by Gas-phase Electron Diffraction

Kinya IJIMA, Eiichi KOSHIMIZU, and Shuzo SHIBATA*

Department of Chemistry, Faculty of Science, Shizuoka University, Oya, Shizuoka 422

(Received December 9, 1981)

The molecular structure of trimethylphosphine-boron triiodide $(\text{CH}_3)_3\text{P}\cdot\text{BI}_3$ has been determined by means of gas-electron diffraction. The molecular parameters and their uncertainties were $r_g(\text{B-I})=2.233\pm0.003$ Å, $r_g(\text{P-B})=1.947\pm0.011$ Å, $r_g(\text{C-P})=1.809\pm0.003$ Å, $r_g(\text{C-H})=1.094\pm0.008$ Å, $\angle\text{IBI}=111.6\pm0.3^\circ$, and $\angle\text{CPC}=106.0\pm0.5^\circ$. The gaseous molecule was rigid with respect to the rotational vibration around the P-B bond.

Trimethylphosphine readily forms complexes with boron trihalides. The molecular structures of the boron trichloride, boron tribromide, and boron triiodide complexes have been determined in the solid phase,¹⁾ and the first two complexes have also been determined in the gas phase.^{2,3)} In the solid phase, the P-B distances of the complexes decrease with the increase in the atomic numbers of halogen atoms in the boron trihalides, though in the gas phase, the P-B distances in the chloro and bromo complexes are nearly equal. On the other hand, the rotational barrier about the P-B bond of $(\text{CH}_3)_3\text{P}\cdot\text{BBr}_3$ ³⁾ is larger than that of $(\text{CH}_3)_3\text{P}\cdot\text{BCl}_3$ ²⁾ in the gas phase. Thus, it is of interest to study the molecular structure of trimethylphosphine-boron triiodide $(\text{CH}_3)_3\text{P}\cdot\text{BI}_3$ in the gas phase in order to determine the P-B bond distance and the rotational barrier about this bond, and to compare the molecular structures of trimethylphosphine complexes with one another.

Experimental

Trimethylphosphine-silver iodide was prepared by the procedure described elsewhere.⁴⁾ The complex was decomposed at 200 °C under a vacuum, and the trimethylphosphine was collected in a trap cooled by liquid nitrogen after the benzene solution of boron triiodide has previously been condensed. The mixture in the trap was warmed up to room temperature and then allowed to react. Activated charcoal was added to the acetone solution of the crude complex, and sublimations were repeated to remove any impurities. The purity of the complex was confirmed by a study of the IR spectra.⁵⁾

In the electron-diffraction experiment, the sample was vaporized at 200 °C through a high-temperature nozzle. The

photographs were taken using an r^3 -sector on Kodak Electron-Image plates at camera distances of 293.5 and 143.6 mm. The accelerating voltage was 40 kV. The exposure times were 12 s for the long camera distance and 21 s for the short camera distance with an electron-beam current of 0.7 μA . The pressure in the diffraction chamber was below 1×10^{-5} Torr (1 Torr=133.322 Pa) during the experiment. The electron wavelength was determined from the diffraction patterns of thallium chloride.⁶⁾ The optical densities of four long camera-distance plates and four short-camera-distance plates were measured at 0.4 mm intervals by means of a digital microphotometer. The electron-diffraction unit and the digital microphotometer used in the present study have been described previously.⁷⁾

Analysis and Results

The scattering intensities were obtained in the ranges of $s=2.5\text{--}16.2$ Å⁻¹ and $7.5\text{--}34.2$ Å⁻¹ from the long- and short-camera-distance plates respectively. The intensities were leveled by means of theoretical backgrounds, and then the intensities for each camera distance were averaged. The elastic and inelastic scattering factors were taken from the tables prepared by Schäfer *et al.*⁸⁾ and by Cromer and Mann⁹⁾ respectively. The inelastic scattering factor for the hydrogen atom was taken from the table by Tavard *et al.*¹⁰⁾

The background curves were drawn smoothly,¹¹⁾ and the molecular intensities thus obtained are shown in Fig. 2.¹²⁾ The experimental radial distribution function,

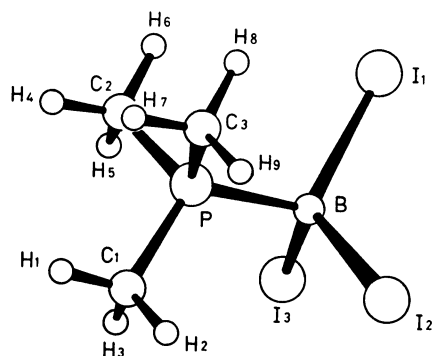


Fig. 1. Numbering of atoms in trimethylphosphine-boron triiodide.

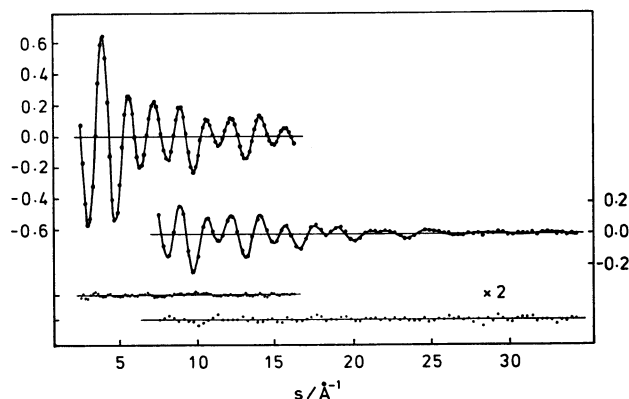


Fig. 2. Molecular intensities for trimethylphosphine-boron triiodide. The upper two curves are long and short camera-distance data. Dots represent observed ones, solid curves calculated ones, and two times the residuals are shown in below.

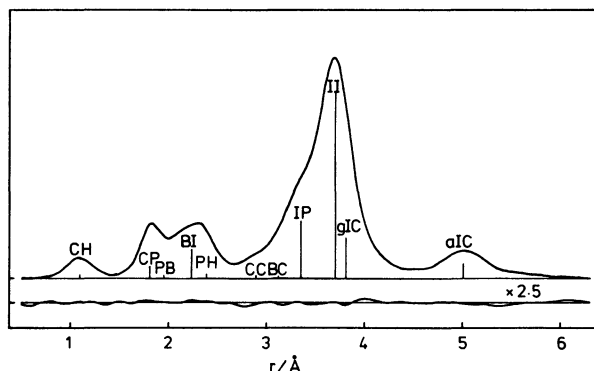


Fig. 3. Radial distribution curve for trimethylphosphine-boron triiodide. Solid curve represents the experimental curve, and lower curve 2.5 times the residuals.

shown in Fig. 3, was calculated from the observed molecular intensities of the range of $s=2.5\text{--}34.2\text{ \AA}^{-1}$, where the long- and the short-camera-distance data were averaged in the overlapped region. A non-nuclear correction for the large difference between the atomic numbers of iodine and the other atom was made.^{13,14)}

The geometrical parameters listed in Table 3 and the mean amplitudes in Table 4 were determined by a least-squares analysis of the molecular intensities. It was assumed that the $(\text{CH}_3)_3\text{P}\cdot\text{BI}_3$ molecule has the C_{3v} symmetry in as staggered form, and that the methyl group has also C_{3v} symmetry in a staggered form with respect to the C-P bond. The asymmetry parameter, κ , for the C-H bond was assumed to be $1.2 \times 10^{-5}\text{ \AA}^3$, given by a diatomic approximation.¹⁵⁾ The asymmetry parameters for the other atomic pairs were neglected. The mean amplitudes and the shrinkage effects,¹⁶⁾ $r_a - r_\alpha$, were calculated on the basis of the force field for $(\text{CH}_3)_3\text{P}\cdot\text{BI}_3$.⁵⁾

The mean amplitudes for the B-I and I...I atomic pairs obtained in the least-squares analysis disagreed with those calculated from the force field given by Drake *et al.*⁵⁾ (see Table 4). On the basis of the fact that

TABLE 1. FORCE FIELD FOR $(\text{CH}_3)_3\text{P}\cdot\text{BI}_3$

$f(\text{CH})$	4.756	$H(\text{BI})$	0.20
$f(\text{HCH})$	0.438	$F(\text{II})$	0.27†
$f(\text{HCP})$	0.639	$F(\text{PI})$	0.18
$f(\text{CPC})$	0.82	$f(\text{CH/CH}')$	0.045
$f(\text{CPB})$	0.99	$f(\text{HCP/HCP}')$	-0.107
$f(\text{CP})$	3.32	$f(\text{CP/CP}')$	0.36
$K(\text{PB})$	2.22	$f(\text{CPB/CPB}')$	-0.045
$K(\text{BI})$	1.2†	$f(\text{PBI/PBI}')$	-0.19
$H(\text{PBI})$	0.22	$Y(\text{CP})$	0.081†

In the present normal-coordinate calculations, the general-valence force constants, f , and the Urey-Bradley force constants, K , H , F , and Y , were used. The units are 10^2 Nm^{-1} for the stretching and repulsion constants, $10^{-18}\text{ J rad}^{-2}$ for the bending constants, and 10^{-18} N m for the torsional constants. The linear constant, F' was assumed to be $-0.1 F$. The values of the force constants were taken from Ref. 5, but those indicated by daggers were estimated for the gaseous molecule in the present study.

TABLE 2. ROOT-MEAN-SQUARE AMPLITUDES AND SHRINKAGE EFFECTS FOR $(\text{CH}_3)_3\text{P}\cdot\text{BI}_3$ (IN 10^{-4} \AA UNITS)

Atomic pair	$l_{\text{calc'd}}$	$r_a - r_\alpha$	Atomic pair	$l_{\text{calc'd}}$	$r_a - r_\alpha$
B-I ₁	721	51	P-C ₁	537	85
P-B	607	39	P...H ₁	1162	317
B...C ₁	1012	71	C ₁ ...C ₂	1085	66
B...H ₁	1244	249	C ₁ -H ₁	784	536
B...H ₂	2132	101	C ₁ ...H ₄	2221	105
I ₁ ...I ₂	1268	-13	C ₁ ...H ₆	2276	82
I ₁ ...P	1264	-6	C ₁ ...H ₆	1265	225
I ₁ ...C ₁	1199	31	H ₁ ...H ₂	1319	833
I ₁ ...C ₂	1997	-35	H ₁ ...H ₄	3134	62
I ₁ ...H ₁	1670	132	H ₁ ...H ₅	3571	-48
I ₁ ...H ₂	1907	86	H ₁ ...H ₆	2271	261
I ₁ ...H ₄	2499	69	H ₂ ...H ₅	2264	244
I ₁ ...H ₆	3150	-92	H ₂ ...H ₆	1521	320
I ₁ ...H ₆	3057	-73	H ₂ ...H ₆	3284	14

The numbering of atoms is shown in Fig. 1.

the force constants of $K(\text{BI})$ and $F(\text{II})$ are mainly related to $l(\text{B-I})$ and $l(\text{I...I})$ respectively, these constants were estimated to be $K(\text{BI})=1.2 \times 10^2\text{ Nm}^{-1}$ and $F(\text{II})=0.27 \times 10^2\text{ Nm}^{-1}$ respectively, so that the calculated values of $l(\text{B-I})$ and $l(\text{I...I})$ might be equal to the respective observed values.

In this calculation, the torsional vibration about the P-B bond was disregarded, for the mean amplitude for the *gauche* I...C atomic pair obtained from the least-squares analysis was nearly equal to that calculated from the force field neglecting this vibration. The force constant for the torsional vibration about the C-P bond was assumed to be $0.08 \times 10^{-18}\text{ N m}$, which was estimated from the potential barrier of 2.6 kcal mol^{-1} for trimethylphosphine.¹⁷⁾ The force constants for gaseous $(\text{CH}_3)_3\text{P}\cdot\text{BI}_3$ modified in the present study are given in Table 1, while the calculated mean amplitudes and the shrinkage corrections for this molecule are given in Table 2.

The r_α parameters determined by the least-squares analysis are listed in Table 3, where the r_g parameters and the limits of error are also listed. The random errors are 2.6 times the standard errors in the least-squares calculations. The systematic errors were estimated from the errors in the measurement of the

TABLE 3. MOLECULAR PARAMETERS OBTAINED FROM LEAST-SQUARES ANALYSIS FOR $(\text{CH}_3)_3\text{P}\cdot\text{BI}_3$

	r_α	r_g	$\epsilon^a)$
B-I	2.226	2.233	0.003
P-B	1.941	1.947	0.011
C-P	1.799	1.809	0.003
C-H	1.035	1.094	0.008
I...I	3.691	3.694	0.004
C...C	2.879	2.890	0.011
$\angle\text{PCH}$	109.2		1.4
$\angle\text{IBI}^b)$	112.0	111.6	0.3
$\angle\text{CPC}^b)$	106.3	106.0	0.5

Bond distance: \AA units; bond angle: degree units.

a) Limits of error. b) Calculated from independent parameters.

TABLE 4. ROOT-MEAN-SQUARE AMPLITUDES FOR $(\text{CH}_3)_3\text{P}\cdot\text{BI}_3$ (IN Å UNIT)

	Obsd ^{a)}	Calcd ^{b)}	Calcd ^{c)}
B-I	0.074 (9)	0.072	0.087
C-P	0.055 (5)	0.054	0.054
C-H	0.075(10)	0.078	0.078
I...I	0.126 (2)	0.122	0.091
I...P	0.111 (5)	0.126	0.128
<i>anti</i> I...C	0.111(14)	0.120	0.125
<i>gauche</i> I...C	0.184(19)	0.199	0.195

a) Results obtained from least-squares analysis of electron-diffraction data. Limits of error are shown in parentheses. b) Values calculated from the force constants in Table 1. c) Values calculated from the force constants in Ref. 5.

camera distance (0.04%) and the wavelength (0.07%). The mean amplitudes, their limits of error, as obtained by least-squares analysis, and the calculated mean amplitudes are listed in Table 4. The correlation matrix is listed in Table 5, while the best-fit theoretical molecular intensities are shown in Fig. 2. The calculations of the mean amplitudes and the shrinkage effects and the

least-squares analysis were carried out on a HITAC M-200H computer in the Computer Center of the University of Tokyo.

Discussion

The molecular parameters for gaseous trimethylphosphine-boron trihalides are listed in Table 6, where the molecular parameters in the solid phase¹⁾ and those for component molecules¹⁸⁻²¹⁾ are also listed. The fractional changes in the parameters, $\Delta f/f$, between the complexes and the component molecules are shown in Fig. 4. The electronegativity of halogen atoms²²⁾ is tentatively taken as the abscissa. It is apparent that, on the complex formation, the $|\Delta f|/f$ ratios systematically increase with the increase in electronegativity, that is, with the decrease in the atomic number of halogen atoms, though the P-B bond distances are equal to each other. On the other hand, the calorimetric study has shown that the complexes are stable in the order of $(\text{CH}_3)_3\text{P}\cdot\text{BF}_3 < (\text{CH}_3)_3\text{P}\cdot\text{BCl}_3 < (\text{CH}_3)_3\text{P}\cdot\text{BBr}_3$,²³⁾ though there are no data for $(\text{CH}_3)_3\text{P}\cdot\text{BI}_3$. These results show that the stability of trimethylphosphine-boron trihalides decreases with an increase in the magnitude

TABLE 5. CORRELATION MATRIX OF $(\text{CH}_3)_3\text{P}\cdot\text{BI}_3$

	$r(\text{BI})$	$r(\text{PB})$	$r(\text{CP})$	$r(\text{CH})$	$r(\text{II})$	$r(\text{CC})$	$\angle\text{PCH}$	$l(\text{BI})$	$l(\text{II})$	$l(\text{IP})$	$l(a\text{IC})$	$l(g\text{IC})$	$l(\text{CP})$	$l(\text{CH})$	$R_1^{a)}$	$R_2^{a)}$
$r(\text{BI})$	1.0															
$r(\text{PB})$	-0.67	1.0														
$r(\text{CP})$	-0.05	0.04	1.0													
$r(\text{CH})$	0.05	-0.02	-0.05	1.0												
$r(\text{II})$	0.30	0.37	-0.13	0.05	1.0											
$r(\text{CC})$	0.02	0.29	0.62	-0.04	0.22	1.0										
$\angle\text{PCH}$	-0.13	0.11	0.09	-0.25	0.05	0.10	1.0									
$l(\text{BI})$	-0.01	0.06	-0.34	-0.05	0.09	-0.23	-0.54	1.0								
$l(\text{II})$	-0.10	-0.11	-0.23	0.04	0.02	-0.32	0.04	0.13	1.0							
$l(\text{IP})$	0.06	0.26	-0.20	0.04	0.66	-0.13	0.16	0.07	0.42	1.0						
$l(a\text{IC})$	0.05	-0.03	-0.09	0.09	0.07	-0.10	-0.18	0.16	0.13	0.08	1.0					
$l(g\text{IC})$	0.32	0.18	-0.21	0.08	0.86	-0.05	-0.01	0.14	0.15	0.73	0.13	1.0				
$l(\text{CP})$	0.42	-0.48	-0.11	0.04	0.01	-0.23	-0.04	-0.01	0.30	0.10	0.09	0.16	1.0			
$l(\text{CH})$	0.07	-0.05	0.00	-0.04	0.08	-0.06	0.00	0.05	0.17	0.13	0.04	0.13	0.19	1.0		
R_1	0.23	-0.08	-0.26	0.15	0.50	-0.39	-0.03	0.18	0.53	0.61	0.21	0.73	0.34	0.19	1.0	
R_2	0.00	0.00	-0.15	0.05	0.14	-0.26	0.03	0.16	0.61	0.31	0.17	0.29	0.34	0.20	0.49	1.0

a) R_1 and R_2 are the indices of resolution for the long- and short-camera-distance data respectively. The indic of resolution and their uncertainties are $R_1=0.93\pm0.02$ and $R_2=0.94\pm0.03$.

TABLE 6. COMPARISON OF MOLECULAR PARAMETERS

	$r(\text{P-B})/\text{\AA}$	$r(\text{B-X})/\text{\AA}$	$r(\text{C-P})/\text{\AA}$	$\angle\text{XBX}/^\circ$	$\angle\text{CPC}/^\circ$
$(\text{CH}_3)_3\text{P}\cdot\text{BCl}_3$ { gas ^{a)}	1.941 (16)	1.851 (7)	1.800 (4)	109.4 (4)	109.3 (3)
solid ^{b)}	1.957 (5)	1.855 (5)	1.80 (1)	111.2 (2)	107.9 (3)
$(\text{CH}_3)_3\text{P}\cdot\text{BBr}_3$ { gas ^{c)}	1.946 (29)	2.010 (9)	1.804 (4)	111.7 (7)	108.0 (7)
solid ^{b)}	1.924 (12)	2.022 (7)	1.81 (1)	110.4 (5)	107.2 (5)
$(\text{CH}_3)_3\text{P}\cdot\text{BI}_3$ { gas ^{d)}	1.947 (11)	2.233 (3)	1.809 (3)	111.6 (3)	106.0 (5)
solid ^{b)}	1.918 (15)	2.249 (12)	1.845 (12)	110.7 (6)	107.8 (6)
$(\text{CH}_3)_3\text{P}^{e)}$			1.846 (3)		98.6 (3)
$\text{BCl}_3^{f)}$		1.742 (4)		120	
$\text{BBr}_3^{g)}$		1.893 (5)		120	
$\text{BI}_3^{h)}$		2.118 (5)		120	

The values in the gas phase represent r_g parameters. The values in parentheses are the limits of error attached to the last significant digits. a) Ref. 2. b) Ref. 1. c) Ref. 3. d) Present study. e) Ref. 18. f) Ref. 19. g) Ref. 20. h) Ref. 21.

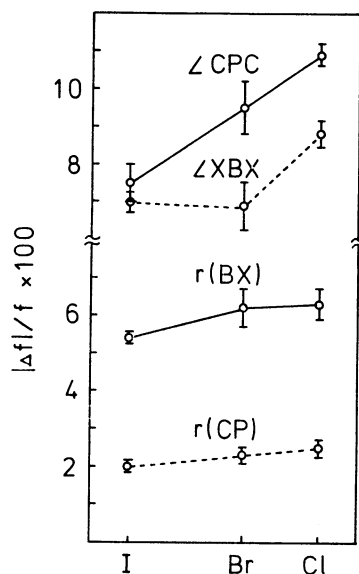


Fig. 4. Parameter changes on complex formation versus electronegativities for halogen atoms. Solid lines represent positive Δf and dashed lines negative Δf .

of the structural changes.

By comparing the parameters of the molecules in the solid phase with those of the gaseous molecules, we see that the dative bonds of $(CH_3)_3P \cdot BBr_3$ and $(CH_3)_3P \cdot BI_3$ seem to be enhanced in the solid phase in the order of $(CH_3)_3P \cdot BBr_3 < (CH_3)_3P \cdot BI_3$, while the dative bond of $(CH_3)_3P \cdot BCl_3$ is unchanged in the solid and gas phases.

The gaseous molecule of $(CH_3)_3P \cdot BI_3$ is rigid with respect to the torsional vibration about the P-B bond, while the potential barriers for $(CH_3)_3P \cdot BCl_3$ ²⁾ and $(CH_3)_3P \cdot BBr_3$ ³⁾ are 3.8 ± 0.7 and about 10 kcal mol⁻¹ respectively. Accordingly, the potential barriers about the P-B bonds of $(CH_3)_3P \cdot BX_3$ are in the order of $(CH_3)_3P \cdot BCl_3 < (CH_3)_3P \cdot BBr_3 < (CH_3)_3P \cdot BI_3$, i.e., in the order of the increasing size of the halogen atoms in the complexes. The height of the rotational barriers of these complexes may be controlled by the repulsion due to the nonbonded atomic pairs, such as $X_1 \cdots H_6$ (see Fig. 1). The $X_1 \cdots H_6$ distances are, however, nearly equal to each other in the above trimethylphosphine complexes; therefore, the above order for the rotational barrier heights is understandable if the large van der Waals radii for halogen atoms with large atomic numbers are taken into consideration.

References

- 1) D. L. Black and R. C. Taylor, *Acta Crystallogr., Sect. B*, **31**, 1116 (1975).
- 2) K. Iijima and S. Shibata, *Bull. Chem. Soc. Jpn.*, **52**, 3204 (1979).
- 3) K. Iijima, E. Koshimizu, and S. Shibata, *Bull. Chem. Soc. Jpn.*, **54**, 2255 (1981).
- 4) R. T. Markham, E. A. Dietz, Jr., and D. R. Martin, *J. Inorg. Nucl. Chem.* **35**, 2659 (1973).
- 5) J. E. Drake, J. L. Hencher, and B. Rapp, *Inorg. Chem.*, **16**, 2289 (1977).
- 6) W. Witt, *Z. Naturforsch., Teil A*, **19**, 1363 (1964).
- 7) S. Shibata, K. Iijima, R. Tani, and I. Nakamura, *Rep. Fac. Sci. Shizuoka Univ.*, **9**, 33 (1974).
- 8) L. Schäfer, A. C. Yates, and R. A. Bonham, *J. Chem. Phys.*, **55**, 3055 (1971).
- 9) D. T. Cromer and J. B. Mann, *J. Chem. Phys.*, **47**, 1892 (1967); D. T. Cromer, *ibid.*, **50**, 4857 (1969).
- 10) C. Tavad, D. Nicolas, and M. Rouault, *J. Chim. Phys.*, **64**, 540 (1967).
- 11) J. Karle and I. L. Karle, *J. Chem. Phys.*, **18**, 957 (1950).
- 12) Numerical experimental data of the leveled total intensity and the background have been deposited with the Chemical Society of Japan (Document No. 8237).
- 13) R. M. Gavin and L. S. Bartell, *J. Chem. Phys.*, **48**, 2460 (1968).
- 14) K. Iijima and S. Shibata, *Bull. Chem. Soc. Jpn.*, **47**, 1393 (1974).
- 15) K. Kuchitsu, *Bull. Chem. Soc. Jpn.*, **40**, 505 (1967).
- 16) K. Kuchitsu and S. J. Cyvin, "Molecular Structures and Vibrations," ed by S. J. Cyvin, Elsevier, Amsterdam (1972), Chap. 12.
- 17) "Kagaku Binran," 2nd ed, ed by the Chemical Society of Japan, Maruzen, Tokyo (1975), p. 1330.
- 18) L. S. Bartell and L. O. Brockway, *J. Chem. Phys.*, **32**, 512 (1960).
- 19) S. Konaka, Y. Murata, K. Kuchitsu, and Y. Morino, *Bull. Chem. Soc. Jpn.*, **39**, 1134 (1966).
- 20) S. Konaka, T. Ito, and Y. Morino, *Bull. Chem. Soc. Jpn.*, **39**, 1146 (1966).
- 21) H. Kakubari, S. Konaka, and M. Kimura, *Bull. Chem. Soc. Jpn.*, **47**, 2337 (1974).
- 22) L. Pauling, "The Nature of the Chemical Bond," 3rd ed, Cornell University Press, Ithaca, New York (1960).
- 23) D. C. Mente, J. L. Mills, and R. E. Mitchell, *Inorg. Chem.*, **14**, 123 (1975); D. C. Mente and J. L. Mills, *ibid.*, **14**, 1862 (1975).